

A NETWORK OF NEUTRAL CURRENT SPHERICAL TPC'S FOR DEDICATED SUPERNOVA DETECTION

Y. Giomataris¹ and J.D. Vergados²

1 CEA, Saclay, DAPNIA, Gif-sur-Yvette, Cedex, France

*2 University of Ioannina, Ioannina, GR 45110, Greece
E-mail: Vergados@cc.uoi.gr*

Abstract

The coherent contribution of all neutrons in neutrino nucleus scattering due to the neutral current offers a realistic prospect of detecting supernova neutrinos. As a matter of fact, for a typical supernova at 10 kpc, about 1000 events are expected using a spherical gaseous detector of radius 4 m and employing Xe gas at a pressure of 10 Atm. We propose a world wide network of several such simple, stable and low cost supernova detectors with a running time of a few centuries.

Key words: PACS numbers:13.15.+g, 14.60Lm, 14.60Bq, 23.40.-s, 95.55.Vj, 12.15.-y.

1 Introduction.

The a typical supernova an energy of about 10^{53} ergs is released in the form of neutrinos [1],[2]. These neutrinos are emitted within an interval of about 10 s after the explosion and they travel to Earth undistorted, except that, on their way to Earth, they may oscillate into other flavors. The phenomenon of neutrino oscillations is by now established by the observation of atmospheric neutrino oscillations [3] interpreted as $\nu_\mu \rightarrow \nu_\tau$ oscillations, as

well as ν_e disappearance in solar neutrinos [4]. These results have been recently confirmed by the KamLAND experiment [5], which exhibits evidence for reactor antineutrino disappearance. Thus for traditional detectors relying on the charged current interactions the precise event rate may depend critically on the specific properties of the supernova, in particular its distance from the Earth. This, of course, may turn into an advantage for the study of the neutrino properties. An additional problem is the fact that the charged current cross sections depend on the details of the structure of the nuclei involved.

In recent years, however, it has become feasible to detect neutrinos by measuring the recoiling nucleus employing gaseous detectors. Thus one is able to explore the advantages offered by the neutral current interaction. This way there are no problems associated with uncertainties in the flux of any neutrino flavor due to oscillations. Furthermore this interaction, through its vector component, can lead to coherence, i.e. an additive contribution of all nucleons in the nucleus. Since the vector contribution of the protons is tiny, the coherence is mainly due to the neutrons of the nucleus.

In this paper we will derive the amplitude for the differential neutrino nucleus coherent cross section. Then we will utilize the available information regarding the energy spectrum of supernova neutrinos and evaluate the expected number of events for all the noble gas targets. Then we will show that these results can be exploited by a network of small and relatively cheap spherical TPC detectors placed in various parts of the world (for a description of the apparatus see our earlier work [6]). The operation of such devices as a network will minimize the background problems. There is no need to go underground, but one may have to go sufficiently deep underwater to balance the high pressure of the gas target. Other types of detectors have also been proposed [7],[8].

Large gaseous volumes are easily obtained by employing long drift technology (i.e TPC) that can provide massive targets by increasing the gas pressure. Combined with an adequate ampli-

fyng structure and low energy thresholds, a three-dimensional reconstruction of the recoiling particle, electron or nucleus, can be obtained. The use of new micropattern detectors and especially the novel Micromegas [9] provide excellent spatial and time accuracy that is a precious tool for pattern recognition and background rejection [10],[11]. The virtue of using such large gaseous volumes and the new high precision microstrip gaseous detectors has been recently discussed in a dedicated workshop [12] and their relevance for low energy neutrino physics and dark matter detection has been widely recognized. Such low-background low-energy threshold systems are actually successfully used in the CAST [13] solar axion experiment and are under development for several low energy neutrino or dark matter projects [6],[14].

2 Elastic Neutrino nucleon Scattering

The cross section for elastic neutrino nucleon scattering has extensively been studied. It has been shown that at low energies it can be simplified and be cast in the form: [1],[15]:

$$\left(\frac{d\sigma}{dT_N}\right)_{weak} = \frac{G_F^2 m_N}{2\pi} [(g_V + g_A)^2 + (g_V - g_A)^2 \left[1 - \frac{T_N}{E_\nu}\right]^2 + (g_A^2 - g_V^2) \frac{m_N T_N}{E_\nu^2}] \quad (2.1)$$

where m_N is the nucleon mass and g_V, g_A are the weak coupling constants. Neglecting their dependence on the momentum transfer to the nucleon they take the form:

$$g_V = -2 \sin^2 \theta_W + 1/2 \approx 0.04, \quad g_A = \frac{1.27}{2}, \quad (\nu, p) \quad (2.2)$$

$$g_V = -1/2, \quad g_A = -\frac{1.27}{2}, \quad (\nu, n) \quad (2.3)$$

In the above expressions for the axial current the renormalization in going from the quark to the nucleon level was taken into

account. For antineutrinos $g_A \rightarrow -g_A$. To set the scale we write:

$$\frac{G_F^2 m_N}{2\pi} = 5.14 \times 10^{-41} \frac{cm^2}{MeV} \quad (2.4)$$

The nucleon energy depends on the neutrino energy and the scattering angle and is given by:

$$T_N = \frac{2 m_N (E_\nu \cos \theta)^2}{(m_N + E_\nu)^2 - (E_\nu \cos \theta)^2}$$

The last equation can be simplified as follows:

$$T_N \approx \frac{2(E_\nu \cos \theta)^2}{m_N}$$

The above formula can be generalized to any target of mass m . It can be written in dimensionless form as follows:

$$y = \frac{2 \cos^2 \theta}{(1 + 1/x)^2 - \cos^2 \theta} \quad , \quad y = \frac{T}{m}, x = \frac{E_\nu}{m} \quad (2.5)$$

The maximum energy occurs when $\theta = 0$ and depends on the neutrino energy (see Fig. 2.1). One can invert the above equation

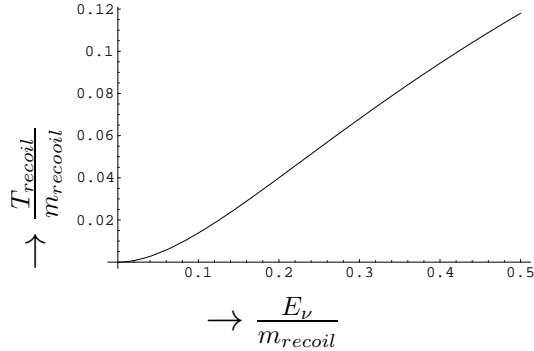


Fig. 2.1. The maximum recoil energy as a function of the neutrino energy (both in units of the recoiling mass)

and get the minimum neutrino energy associated with a given recoil energy. This is useful in obtaining the differential cross section (with respect to the recoil energy) after folding with the

neutrino spectrum. One finds:

$$x = \left[-1 + \sqrt{1 + \frac{2}{y}} \right]^{-1} \quad (2.6)$$

This is shown in Fig. 2.2

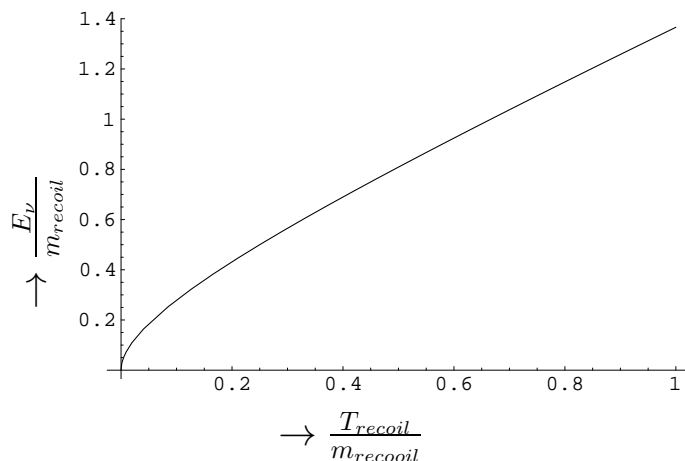


Fig. 2.2. The minimum neutrino energy as a function of the recoil energy (both in units of the recoiling mass)

3 Coherent neutrino nucleus scattering

From the above expressions we see that the vector current contribution, which may lead to coherence, is negligible in the case of the protons. Thus the coherent contribution [16] may come from the neutrons and is expected to be proportional to the square of the neutron number. The neutrino-nucleus scattering can be obtained from the amplitude of the neutrino nucleon scattering under the following assumptions:

- Employ the appropriate kinematics, i.e. those involving the elastically scattered nucleus.
- Ignore effects of the nuclear form factor. Such effects, which are not expected to be very large, are currently under study and they will appear elsewhere.

- The effective neutrino-nucleon amplitude is obtained as above with the substitution

$$\mathbf{q} \Rightarrow \frac{\mathbf{p}}{A} \quad , \quad E_N \Rightarrow \sqrt{m_N^2 + \frac{\mathbf{p}^2}{A^2}} = \frac{E_A}{A}$$

with \mathbf{q} the nucleon momentum and \mathbf{p} the nuclear momentum.

Under the above assumptions the neutrino-nucleus cross section takes the form:

$$\begin{aligned} \left(\frac{d\sigma}{dT_A} \right)_{weak} &= \frac{G_F^2 A m_N}{2\pi} [(M_V + M_A)^2 \left(1 + \frac{A-1}{A} \frac{T_A}{E_\nu} \right) \\ &+ (M_V - M_A)^2 \left(1 - \frac{T_A}{E_\nu} \right)^2 \left(1 - \frac{A-1}{A} \frac{T_A}{m_N E_\nu / T_A - 1} \right) \\ &+ (M_A^2 - M_V^2) \frac{A m_N T_A}{E_\nu^2}] \end{aligned} \quad (3.7)$$

Where M_V and M_A are the nuclear matrix elements associated with the vector and the axial current respectively and T_A is the energy of the recoiling nucleus. The axial current contribution vanishes for $0^+ \Rightarrow 0^+$ transitions. Anyway it is negligible in front of the coherent scattering due to neutrons. Thus the previous formula is reduced to:

$$\begin{aligned} \left(\frac{d\sigma}{dT_A} \right)_{weak} &= \frac{G_F^2 A m_N}{2\pi} (N^2/4) F_{coh}(A, T_A, E_\nu), \\ F_{coh}(A, T_A, E_\nu) &= \left(1 + \frac{A-1}{A} \frac{T_A}{E_\nu} \right) + \left(1 - \frac{T_A}{E_\nu} \right)^2 \\ &\left(1 - \frac{A-1}{A} \frac{T_A}{m_N E_\nu / T_A - 1} \right) - \frac{A m_N T_A}{E_\nu^2} \end{aligned} \quad (3.8)$$

The function $F_{coh}(A, T_A, E_\nu)$ is shown in Fig 3.3 as a function of the recoil energy in the case of Ar and Xe for 10, 20, 30 and 40 MeV respectively.

We see two reasons for enhancement of the cross section:

- The overall A factor due to the kinematics, which is counter-

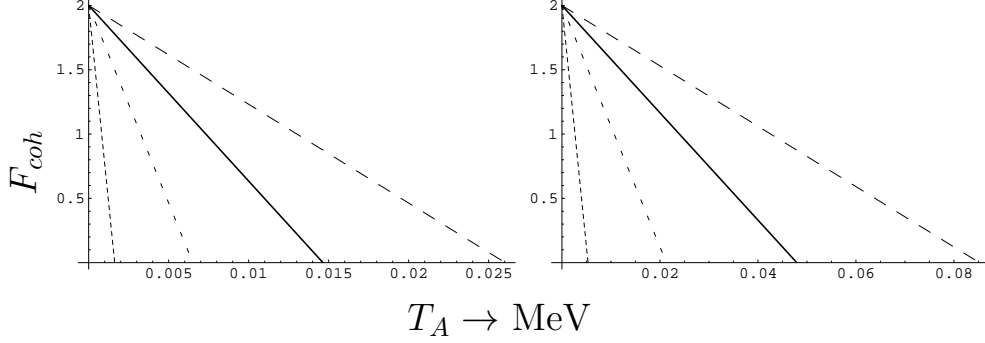


Fig. 3.3. The function $F_{coh}(A, T_A, E_\nu)$ as a function of the recoil energy T_A for, from left to right, $E_\nu = 10, 20, 30, 40$ MeV. The results shown are for Xe on the left and Ar on the right

acted by the smaller nuclear recoil energy when compared to the nucleon recoil energy for the same neutrino energy. This factor will be absorbed into the energy integrals, see the function $F_{fold}(A, T, (T_A)_{th})$ below.

- The N^2 enhancement due to coherence.

4 Supernova Neutrinos

The number of neutrino events for a given detector depends on the neutrino spectrum and the distance of the source. We will consider a typical case of a source which is about 10 kpc, i.e. $D = 3.1 \times 10^{22}$ cm with an energy output of 3×10^{53} ergs with a duration of about 10 s. We will further assume that the energy is shared equally by each neutrino flavor. Furthermore each neutrino flavor is characterized by a Fermi-Dirac like distribution times its characteristic cross section, i.e $U_\nu = 0.5 \times 10^{53}$ ergs per neutrino flavor, i.e.

$$\frac{dN}{dE_\nu} = \sigma(E_\nu) \frac{E_\nu^2}{1 + \exp(E_\nu/T)} = \frac{\Lambda}{JT} \frac{x^4}{1 + e^x} \quad (4.9)$$

with $J = \frac{31\pi^6}{252}$, Λ a constant and T the temperature of the emitted neutrino flavor. Each flavor is characterized by its own tempera-

ture as follows:

$$T = 8 \text{ MeV for } \nu_\mu, \nu_\tau, \tilde{\nu}_\mu, \tilde{\nu}_\tau \text{ and } T = 5 \text{ (3.5) MeV for } \tilde{\nu}_e (\nu_e)$$

The constant Λ is determined by the requirement that the distribution yields the total energy of each neutrino species.

$$U_\nu = \frac{\Lambda T}{J} \int_0^\infty dx \frac{x^5}{1 + e^x} \Rightarrow \Lambda = \frac{U_\nu}{T}$$

Thus one finds:

$$\Lambda = 0.89 \times 10^{58} (\nu_e), 0.63 \times 10^{58} (\tilde{\nu}_e), 0.39 \times 10^{58} \text{ (all other flavors)}$$

The emitted neutrino spectrum is shown in Fig. 4.4.

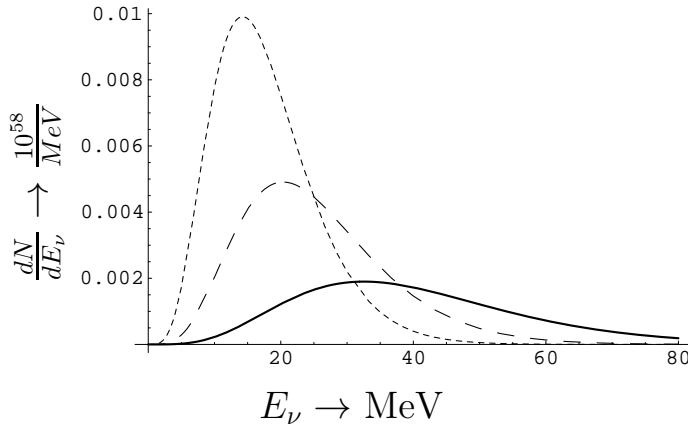


Fig. 4.4. The supernova neutrino spectrum. The short dash, long dash and continuous curve correspond to $\nu_e, \tilde{\nu}_e$ and all other flavors respectively

The differential event rate (with respect to the recoil energy) is proportional to the quantity:

$$\frac{dR}{dT_A} = \frac{\lambda(T)}{J} \int_0^\infty dx F_{coh}(A, T_A, xT) \frac{x^4}{1 + e^x} \quad (4.10)$$

with $\lambda(T) = (0.89, 0.63, 0.39)$ for $\nu_e, \tilde{\nu}_e$ and all other flavors respectively. This is shown in Figs. 4.5 and 4.5. The total number of expected events for each neutrino species can be cast in the form:

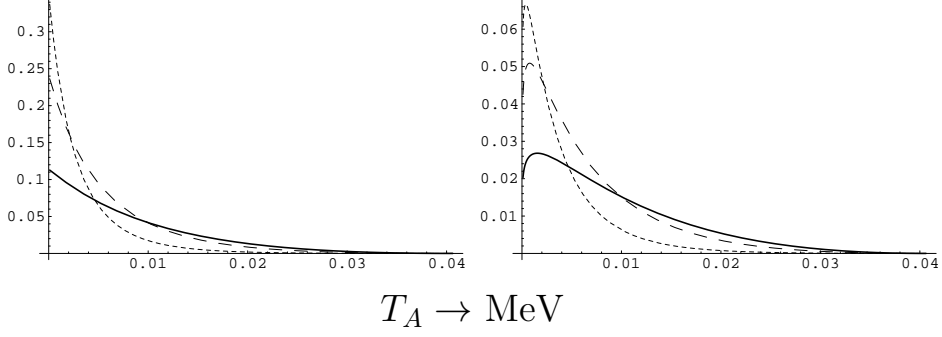


Fig. 4.5. The differential event rate as a function of the recoil energy T_A , in arbitrary units, for Xe. On the left we show the results without quenching, while on the right the quenching factor is included. We notice that the effect of quenching is more prevalent at low energies. The notation for each neutrino species is the same as in Fig. 4.4

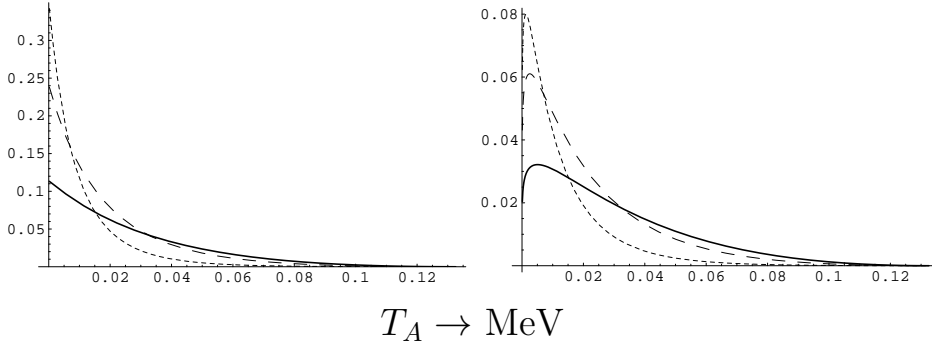


Fig. 4.6. The same as in Fig. 4.5 for the Ar target.

$$\text{No of events} = \tilde{C}_\nu(T) h(A, T, (T_A)_{th}), \quad (4.11)$$

$$h(A, T, (T_A)_{th}) = \frac{F_{fold}(A, T, (T_A)_{th})}{F_{fold}(40, T, (T_A)_{th})} \quad (4.12)$$

with

$$F_{fold}(A, T, (T_A)_{th}) = \frac{A}{J} \int_{(T_A)_{th}}^{(T_A)_{max}} \frac{dT_A}{1 \text{MeV}} \times \int_0^\infty dx F_{coh}(A, T_A, xT) \frac{x^4}{1 + e^x} \quad (4.13)$$

and

$$\tilde{C}_\nu(T) = \frac{G_F^2 m_N 1 \text{MeV}}{2\pi} \frac{N^2}{4} \Lambda(T) \frac{1}{4\pi D^2} \frac{PV}{kT_0} \quad (4.14)$$

Where k is Boltzmann's constant, P the pressure, V the volume, and T_0 the temperature of the gas.

Summing over all the neutrino species we can write:

$$\text{No of events} = C_\nu r(A) \frac{K(A, (T_A)_{th})}{K(40, (T_A)_{th})} Qu(A) \quad (4.15)$$

with

$$C_\nu = 153 \left(\frac{N}{22}\right)^2 \frac{U_\nu}{0.5 \times 10^{53} \text{ergs}} \left(\frac{10 \text{kpc}}{D}\right)^2 \frac{P}{10 \text{Atm}} \left[\frac{R}{4m}\right]^3 \frac{300}{T_0} \quad (4.16)$$

In the above expression $r(A)$ is a kinematical parameter depending on the nuclear mass number, which is essentially unity.

$K(A, (T_A)_{th})$ is the rate at a given threshold energy divided by that at zero threshold. It depends on the threshold energy, the assumed quenching factor and the nuclear mass number. It is unity at $(T_A)_{th} = 0$. The function $r(A)$ is plotted in 4.7. It is seen that it can be well approximated by unity.

From the above equation we find that, ignoring quenching, the following expected number of events:

$$1.25, 31.6, 153, 614, 1880 \text{ for He, Ne, Ar, Kr and Xe} \quad (4.17)$$

respectively. For other possible targets the rates can be found by the above formulas or interpolation.

The function $K(A, (T_A)_{th})$ is plotted in Fig. 4.8 for threshold energies up to 2keV. We see that the threshold effects are stronger in heavier systems since, on the average, the transferred energy is smaller. Thus for a threshold energy of 2 keV in the case of Xe the number of events is reduced by 30% compared to those at zero threshold.

The quantity $Qu(A)$ is a factor less than one multiplying the total rate, assuming a threshold energy $(T_A)_{th} = 100\text{eV}$, due to the quenching. The idea of quenching is introduced, since, for low energy recoils, only a fraction of the total deposited energy goes

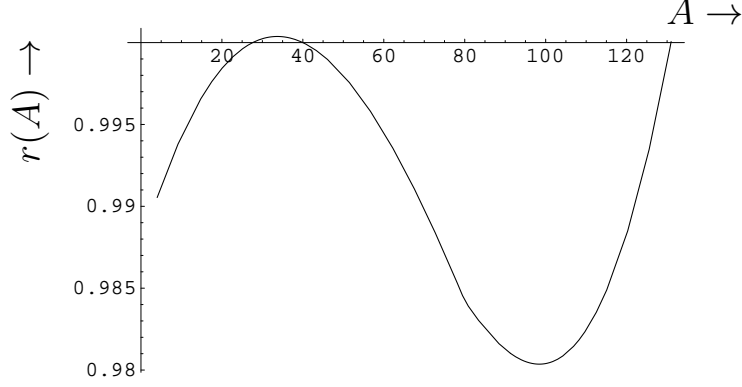


Fig. 4.7. The function $r(A)$ versus the nuclear mass number. To a good approximation $r(A) \simeq 1.0$ (for definitions see text)

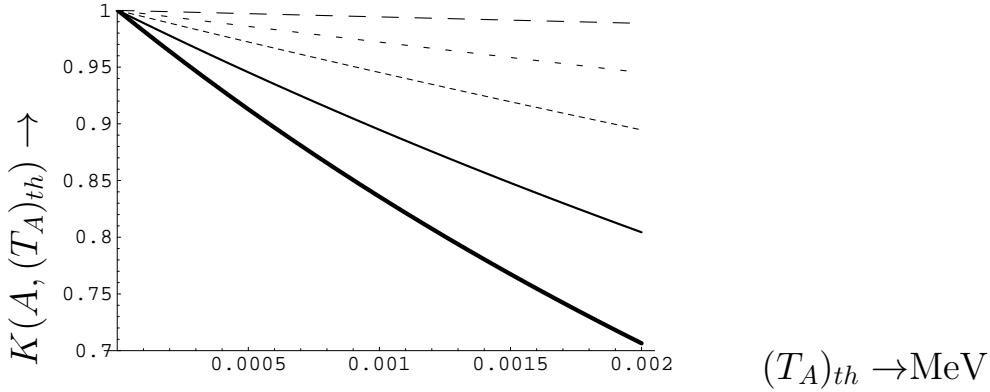


Fig. 4.8. The function $K(A, (T_A)_{th})$ versus $(T_A)_{th}$ for various the nuclear mass numbers without the quenching factor. From top to bottom He, Ne, Ar, Kr and Xe. (for definitions see text)

into ionization. The ratio of the amount of ionization induced in the gas due to nuclear recoil to the amount of ionization induced by an electron of the same kinetic energy is referred to as a quenching factor Q_{fac} . This factor depends mainly on the detector material, the recoiling energy as well as the process considered [17]. In our estimate of $Qu(T_A)$ we assumed a quenching factor of the following empirical form motivated by the Lidhard theory [17]-[18]:

$$Q_{fac}(T_A) = r_1 \left[\frac{T_A}{1keV} \right]^{r_2}, \quad r_1 \simeq 0.256, \quad r_2 \simeq 0.153 \quad (4.18)$$

Then the parameter $Qu(A)$ takes the values:

$$0.49, 0.38, 0.35, 0.31, 0.29 \text{ for He, Ne, Ar, Kr and Xe} \quad (4.19)$$

respectively. The effect of quenching is larger in the case of heavy targets, since, for a given neutrino energy, the energy of the recoiling nucleus is smaller. Thus the number of expected events for Xe assuming a threshold energy of 100 eV is reduced to about 560.

The effect of quenching is exhibited in Fig 4.9 for the two interesting targets Ar and Xe.

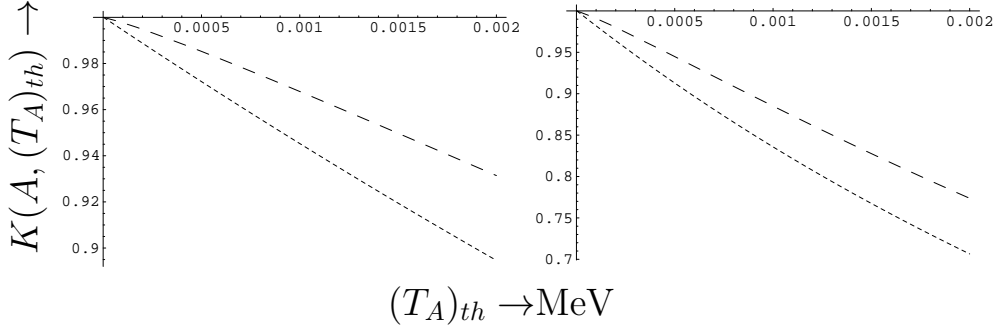
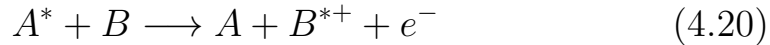


Fig. 4.9. The function $K(A, (T_A)_{th})$ versus $(T_A)_{th}$ for the target Ar on the left and Xe on the right. The short and long dash correspond to no quenching and quenching factor respectively. One sees that the effect of quenching is less pronounced at higher thresholds. The differences appear small, since we present here only the ratio of the rates to that at zero threshold. The effect of quenching at some specific threshold energy is not shown here. For a threshold energy of 100 eV the rates are quenched by factors of 3 and 3.5 for Ar and Xe respectively (see Eq. (4.19)).

We should mention that it is of paramount importance to experimentally measure the quenching factor. The above estimates were based on the assumption of a pure gas. In our detection scheme the Xe gas carrier (A) is mixed with a small fraction of low ionization potential gas (B). Thus a part of the excitations produced on the Xe atoms could be transferred to ionization through the well known Penning effect as follows:



Such an effect will lead to an increase in the quenching factor and needs be measured.

5 The NOSTOS detector network

A description of the NOSTOS project and details of the spherical TPC detector are given in [6]. We have built a spherical prototype 1.3 m in diameter which is described in [19]. The outer vessel is made of pure Cu (6 mm thick) allowing to sustain pressures up to 5 bar. The inner detector is just a small sphere, 10 mm in diameter, made of stainless steel as a proportional counter located at the center of curvature of the TPC. We intend to use as amplifying structure a spherical TPC [20] and developments are currently under way to build a spherical TPC detector using new technologies. First tests were performed by filling the volume with argon mixtures and are quite promising. High gains are easily obtained and the signal to noise is large enough for sub-keV threshold. The whole system looks stable and robust. The advantages of using the spherical detector concept are the following;

- (1) The natural radial focusing of the TPC allows to collect and amplify the deposited charges by a simple and robust detector using a single electronic channel to read out a large gaseous volume. The small size associated to small detector capacitance permits one to achieve very low electronic noise. In the present prototype the noise is as low as a few hundred electrons and has easily been obtained; with optimized low noise amplifiers we hope to lower it to the level of a few tenths. This is a key point for the obtaining a very low energy threshold, i.e. down to 100 eV, by operating the detector at moderate gain of about 100. Such low gains are easily obtained at atmospheric pressure and open the way to operate the TPC at high pressures. We target pressures as high as 10 bar for Xenon gas. Even higher pressures by a factor 3-6 are aimed in the case of Argon gas in order to achieve, to first order, the same number of events.
- (2) The radial electric field, inversely proportional to the square of the radius, is a crucial point for measuring the depth of the

interaction by a simple analysis of the time structure of the detector signal. A position resolution of about 10 cm has been already obtained, a fact that is of paramount importance for improving the time resolution of the detector and rejecting background events by applying fiducial cuts.

- (3) Building a high pressure metallic sphere, for instance made out of stainless steel or copper, seems to assure an excellent quality of the gas mixture and turns out that a single gas filling with pure gas is sufficient to maintain the stability of the signal for several months. We are pushing the technology to improve the properties of the various elements in order to achieve stability over many years.
- (4) Big high pressure-secure tanks are under development by many international companies for hydrogen or oil storage, and therefore the main element of the TPC could be shipped at moderate cost.

Our idea is then to build several such low cost and robust detectors and install them in several places over the world. First estimations show that the required background level is modest and therefore there is not need for deep underground laboratory. A mere 100 meter water equivalent coverage seems to be sufficient to reduce the cosmic muon flux at the required level (in the case of many such detectors in coincidence, a modest shield is sufficient). The maintenance of such system could be easily assured by Universities or even by secondary schools. Thanks to the simplicity of the system it could be operated by young students with a specific running program and simple maintenance every a few years. Notice that such detector scheme, measuring low energy nuclear recoils from neutrino nucleus elastic scattering, do not determine the incident neutrino vector and therefore it is not possible this way to localize the Supernova. A cluster of such detectors in coincidence, however, could localize the star by a triangulation technique.

A network of such detectors in coincidence with a sub-keV threshold could also be used to observe unexpected low energy events.

This low energy range has never been explored using massive detectors. A challenge of great importance will be the synchronization of such a detector cluster with the astronomical γ -ray burst telescopes to establish whether low energy recoils are emitted in coincidence with the mysterious γ bursts.

6 Conclusions

In the present study it has been shown that it is quite simple to detect typical supernova neutrinos in our galaxy. The idea is to employ a small size spherical TPC detector filled with a high pressure noble gas. An enhancement of the neutral current component is achieved via the coherent effect of all neutrons in the target. Thus employing, e.g., Xe at 10 Atm, with a feasible threshold energy of about 100 eV in the detection the recoiling nuclei, one expects between 600 and 1900 events, depending on the quenching factor. We believe that networks of such dedicated detectors, made out of simple, robust and cheap technology, can be simply managed by an international scientific consortium and operated by students. This network comprises a system, which can be maintained for several decades (or even centuries). This is a key point towards being able to observe few galactic supernova explosions.

acknowledgments: This work was supported in part by the European Union under the contracts RTN No HPRN-CT-2000-00148 and MRTN-CT-2004-503369.

References

- [1] J.F. Beacom, W.M. Farr and P. Vogel, Phys. Rev D **66** (2002) 033001;hep-ph/0205220
- [2] J.R. Wilson and R.W. Mayle, Phys. Rept. **227** (1993) 97.
M. Herant, W. Benz, W.R. Hix, C.L. Fryer and S.A. Golgate, Astrophys. J. **435** (1994) 339.
M. Rampp and H.T. Janka, Astrophys. J. **539** (2000) L33.
A. Mezzacappa, M. Liebendorfer, O.E. Messer, W.R. Hix, F.K. Thielemann and S.W. Bruenn, Phys. Rev. Lett. **86** (2001) 1935.
C.L. Fryer and A. Heger Astrophys. J. **541** (2000) 1033.
G.G. Raffelt, Nuc. Phys. Proc. Suppl. **110** (2002) 254;hep-ph/0201099;
R. Tomas, M. Kachelriess, G.G. Raffelt, A. Dighe, A-T Janka and L. Schreck, JCAP **0409** (2004) 015;
R. Tomas, D. Semikoz, G.G. Raffelt, M. Kachelriess and A.S. Dighe, Phys. Rev. D **68** (2002) 093013;

- M.T. Keil, G.G. Raffelt, A-T Janka, *Astrophys. J.* **590** (2003) 971;
 J.F. Beacom, R.N. Boyd and A. Mezzacappa, *Phys. Rev. D* **63** (2001) 073011.
 M.K. Sharp, J.F. Beacom J.A. Formaggio, *Phys. Rev. D* **66** (2002) 013012; hep-ph/0205035.
 A. Burrows, J. Hayes and B.A. Fryxell, *Astrophys. J.* **450** (1995) 830.
- [3] Y. Fukuda *et al*, The Super-Kamiokande Collaboration, *Phys. Rev. Lett.* **86**, (2001) 5651; *ibid* **81** (1998) 1562 & 1158; *ibid* **82** (1999) 1810 ;*ibid* **85** (2000) 3999.
- [4] Q.R. Ahmad *et al*, The SNO Collaboration, *Phys. Rev. Lett.* **89** (2002) 011302; *ibid* **89** (2002) 011301 ; *ibid* **87** (2001) 071301.
 K. Lande *et al*, Homestake Collaboration, *Astrophys. J* **496**, (1998) 505
 W. Hampel *et al*, The Gallex Collaboration, *Phys. Lett. B* **447**, (1999) 127;
 J.N. Abdurashitov *al*, Sage Collaboration, *Phys. Rev. C* **80** (1999) 056801;
 G.L Fogli *et al*, *Phys. Rev. D* **66** (2002) 053010.
- [5] K. Eguchi *et al*, The KamLAND Collaboration, *Phys. Rev. Lett.* **90** (2003) 021802, hep-exp/0212021.
- [6] Y. Giomataris and J.D. Vergados, *Nucl. Instr. Meth. A* **53** (2004) 330.
- [7] P. Barbeau, J.I. Collar, J. Miyamoto and I. Shipsey, *IEEE Trans. Nucl. Sci.* **50** (2003) 1285.
- [8] C. Haggmann and A. Bernstein, *IEEE Trans. Nucl. Sci.* **51** (2004) 2151.
- [9] I. Giomataris *et al.*, *Nucl. Instr. Meth. A* **376** (1996) 29
- [10] J.I. Collar and Y. Giomataris, *Nucl. Inst. Meth.* **471** (2001) 254
- [11] P. Gorodetzky *et al.*, *Nucl.Phys.Proc.Suppl.* **138** (2005) 56
- [12] Spherical TPC Workshop, Paris 2004
- [13] C.E. Aalseth *et al.*, *Nucl.Phys.Proc.Suppl.* **110** (2002) 85.
- [14] I. Giomataris *et al.*, hep-ex/0502033.
 T. Patzak *et al.*, *Nucl. Instr. Meth. A* **434** (1999) 358.
 B. Ahmed, G. J. Alner, H. Araujo, J. C. Barton, A. Bewick, M. J. Carson, D. Davidge, J. V. Dawson, T. Gamble, S. P. Hart, R. Hollingworth, A. S. Howard, W. G. Jones, M. K. Joshi, V. A. Kudryavtsev, T. B. Lawson, V. Lebedenko, M. J. Lehner, J. D. Lewin, P. K. Lightfoot, I. Liubarsky, R. Luscher, J. E. McMillan, B. Morgan, G. Nicklin, S. M. Paling, R. M. Preece, J. J. Quenby, J. W. Roberts, M. Robinson, N. J. T. Smith, P. F. Smith, N. J. C. Spooner, T. J. Sumner, D. R. Tovey, *Astropart.Phys.* **19** (2003).
- [15] P. Vogel and J. Engel, *Phys. Rev. D* **39** (1989) 3378.
- [16] E.A. Paschos and A. Kartavtsev, hep-ph/0309148.
- [17] E. Simon *et al*, *Nucl. Instr. Meth. A* **507** (2003) 643; astro-ph/0212491.
- [18] J. Lidhart *et al*, *Mat. Phys. Medd. Dan. Vid. Selsk.* **33** (10) (1963) 1

- [19] The NOSTOS experiment and new trends in rare event detection, I. Giomataris et al, hep-ex/0502033, submitted to the SIENA2004 International Conference (2005).
- [20] Y. Giomataris, P. Rebourgeard, J.P. Robert, Georges Charpak, Nucl. Instrum. Meth. A **376** (1996) 29